Journal of Neuroscience Research 00:00–00 (2014)

Astrocytic Exportin-7 Responds to Ischemia Through Mediating LKB1 Translocation From the Nucleus to the Cytoplasm

Hai Jie Liang,[1,2] Rui Chao Chai,[1,2,3] Xi Li,[1,2] Jin Ge Kong,[1,2] Jiao Hua Jiang,[1,2] Ju Ma,[1,2] Greg Vatcher,[1,2,3] and Albert Cheung Hoi Yu[1,2,3,4]★

[1]Neuroscience Research Institute and Department of Neurobiology, School of Basic Medical Sciences, Peking University, Beijing, China
[2]Key Laboratory for Neuroscience of the Ministry of Education and Key Laboratory for Neuroscience of the National Health and Family Planning Commission, Peking University, Beijing, China
[3]Hai Kang Life Corporation Limited, Beijing, China
[4]Laboratory of Translational Medicine, Institute of Systems Biomedicine, Peking University, Beijing, China

The superfamily of importin-β–related proteins is the largest class of nuclear transport receptors and can be generally divided into importins and exportins according to their transport directions. Eleven importins and seven exportins have been identified, and the expression patterns of both classes are important for their functions in nucleocytoplasmic transport activities. This study demonstrates that all of the importins (importin-β; transportin-1, -2, and -3; and importin-4, -5, -7, -8, -9, -11, and -13) and all the exportins (exportin-1, -2, -4, -5, -6, -7, and -t) are differentially expressed in the cerebral cortex, cerebellum, hippocampus, and brainstem and in primary cultures of cerebral cortical astrocytes and neurons. For astrocytes, we observed that different importins and exportins displayed different expression changes during 0–6 hr of ischemia treatment, especially an increase of both the mRNA and the protein of exportin-7. Immunostaining showed that exportin-7 accumulated inside the nucleus and around the nuclear envelope. In addition, we noticed an increased cytoplasmic distribution of one of the cargo proteins of exportin-7, LKB1, an important element in maintaining energy homeostasis. This increased cytoplasmic distribution was accompanied by an increased expression of exportin-7 under ischemia in astrocytes. We demonstrate that exportin-7 responds to ischemia in astrocytes and that this response involves translocation of LKB1, a protein that plays important roles during metabolic stress, from the nucleus to the cytoplasm.

Key words: exportins; importins; brain metabolic injury; nucleocytoplasmic transport; LKB1

The nucleocytoplasmic transport of macromolecules larger than 40–60 kDa is mediated mainly by the superfamily of importin-β–related proteins, which are generally divided into importins and exportins according to their transport directions (Fried and Kutay, 2003; Mingot et al., 2004; You et al., 2013). The subfamily of importins includes importin-β, -4, -5, -6, -7, -8, -9, -11, and -13 and transportin-1, -2, and -3, and the subfamily of exportins includes exportin-1, -2, -t, -4, -5, -6, and -7 (Fried and Kutay, 2003; Guttler and Gorlich, 2011).

The expression levels of importins and exportins in a cell or an organ are highly related to their functions in each cell or organ, inasmuch as different importing or

Additional Supporting Information may be found in the online version of this article.

H.J. Liang, R.C. Chai, and X. Li contributed equally to this work.

This article was published online on 24 September 2014. An error was subsequently identified. This notice is included in the online and print versions to indicate that both have been corrected on 30 September 2014.

Contract grant sponsor: Beijing Natural Science Foundation; Contract grant number: 7091004; Contract grant sponsor: National Basic Research Program of China (973 Program); Contract grant number: 2011CB504400; Contract grant sponsor: National Natural Science Foundation of China; Contract grant number: 30870818; Contract grant number: 31070974; Contract grant number: 31171009; Contract grant number: 81471253; Contract grant sponsor: Foundation for Innovative Research Groups of the National Natural Science Foundation of China; Contract grant number: 81221002; Contract grant sponsor: National Fund for Fostering Talents of Basic Science; Contract grant number: J1030831 (to H.J.L., X.L); Contract grant number: J0108 (to H.J.L., X.L.).

★Correspondence to: Albert Cheung Hoi Yu, PhD, Neuroscience Research Institute, Peking University, 38 Xue Yuan Road, Beijing 100191, China. E-mail: achy@hsc.pku.edu.cn

Received 8 March 2014; Revised 16 July 2014; Accepted 18 August 2014

Published online 00 Month 2014 in Wiley Online Library (wileyonlinelibrary.com). DOI: 10.1002/jnr.23486

exporting activities are dependent on the amounts of importins and exportins (Hosokawa et al., 2008; You et al., 2013). In the central nervous system (CNS), expression level changes in importins and exportins have been reported to be involved in neuronal cell differentiation and embryonic development (Grunwald et al., 2013; You et al., 2013). In addition, expression changes of importins and exportins are also involved in various CNS functions, dysfunctions, and injuries, such as neuronal differentiation, axonal injury and functional recovery, neuronal plasticity formation, and pathogenesis of amyotrophic lateral sclerosis (ALS; Hanz et al., 2003; Yasuhara et al., 2007; Deng et al., 2009; Nagara et al., 2013).

Ischemia injury is common in the brain; it is the second most frequent cause of death and major disability in the world (Dong et al., 2010; Xu et al., 2012; Bai and Li, 2013). Our previous study (Chen et al., 2003) identified that 14-3-3γ and exportin-7 (unpublished data) mRNA expression increased in astrocytes under ischemia treatment. Exportin-7 was first discovered and identified as a novel RanGTP-binding protein by two different groups (Koch et al., 2000; Kutay et al., 2000). It was shown to bind RanGTP and prevent hydrolysis, directly interact with nucleoporins, and enter the nucleus without other soluble transport factors in HeLa cells (Kutay et al., 2000). Exportin-7 can mediate nuclear export of p50RhoGAP and 14-3-3σ in a process dependent on nuclear export signals that differ fundamentally from the classic leucine-rich exportin-1-dependent signals (Mingot et al., 2004). Exportin-7 also interacts with the basic helix-loop-helix transcription factor E12 and enhances its transcriptional activity (Lee et al., 2010). In addition, exportin-7 is responsible for the nuclear export of LKB1, a master kinase that controls at least 13 downstream protein kinases, including the adrenosine monophosphate (AMP)-activated protein kinase (Dorfman and Macara, 2008). LKB1 is also critically important in mediating energy homeostasis in response to energy stress (Shaw et al., 2004, 2005; Ohashi et al., 2010).

This study clarifies the mRNA expression patterns of the importins and exportins in the cerebral cortex, cerebellum, hippocampus, and brainstem of adult mice; in primary cultures of neurons and astrocytes; and in primary culture of astrocytes under 0–6 hr of ischemia treatment. The results indicate that upregulation of exportin-7 in astrocytes under ischemia might facilitate nuclear export of LKB1, which might help astrocytes respond to ischemic insult.

MATERIALS AND METHODS

Primary Cultures of Astrocytes and Neurons

Primary cultures of cerebral cortical astrocytes were prepared from newborn ICR mice as previously described (Yu et al., 1982; Yu and Lau, 2000; Chen et al., 2003; Jiang et al., 2003; Yang et al., 2011; Chai et al., 2013). Cerebral cortices were carefully dissected from the brains and cut into small pieces (<1 mm^3) in ice-cold Dulbecco's modified Eagle's medium (DMEM; Gibco, Life Technologies, Gaithersville, MD). After undergoing vortexing for 1.5 min at 2,000 rpm to dissociate the cells mechanically, the cell suspension was sequentially passed through 70- and 10-μm sterile nylon filters (Spectra/Mesh; SpectrumLabs, Rancho Dominguez, CA). Fetal bovine serum (FBS; HyClone, Australia) was added (to 10% in the final volume) and the mixture was plated in 35-mm Falcon tissue culture dishes at 4×10^5 cell/ml (Becton Dickinson, Franklin Lakes, NJ). Cultures were kept in a 37°C, 5% CO_2 incubator and were fed twice weekly with DMEM and 10% FBS for the first 2 weeks and then DMEM, 7% FBS for the following 2 weeks. Cultured astrocytes were used for experiments 4 weeks after being seeded.

Primary cultures of cortical neurons were prepared from embryonic ICR mice as described previously (Z. Li et al., 2001; Q. Li et al., 2002; Chen et al., 2005c). Cytosine arabinoside (40 μM; Sigma-Aldrich, St. Louis, MO) was added on day 3 to inhibit the growth of the astrocytes. Cultured neurons were used on day 7 (Yu et al., 1984).

Acute Isolation of Brain Tissues

Nine-week-old mice (male) were anesthetized with chloral hydrate (350 mg/kg; Sigma-Aldrich) and perfused with phosphate-buffered saline (PBS) to remove all the blood. Brains were carefully isolated from the cranium and dissected in ice-cold PBS. Tissues of the cerebral cortex, cerebellum, hippocampus, and brainstem were dissected and frozen in liquid nitrogen immediately before being stored at −80°C.

Anaerobic Chamber-Induced Ischemia

In vitro ischemia was induced by using a Forma anaerobic chamber (85% N_2, 10% H_2, and 5% CO_2 at 37°C; Thermo Fisher Scientific, Waltham, MA) as previously described (Yu et al., 2001, 2003, 2007; Chen et al., 2005a; Dong et al., 2009; Zhou et al., 2010; Chai et al., 2013). Briefly, the medium used for the ischemia experiment was glucose and serum-free DMEM, equilibrated overnight in an anaerobic chamber. Cultures were first washed twice with ischemic medium and then incubated with 0.8 ml ischemic medium per 35-mm culture dish for 0.5, 1, 2, 4, and 6 hr in the anaerobic chamber.

The mineral oil ischemia model previously described by Yu et al. (1995) was used for studying astrocytes via microscopy. Briefly, after undergoing ischemia treatment for 30 min with anaerobic chamber-induced ischemia, the medium was changed with 2 ml of glucose-free HEPES buffer saturated with nitrogen for 30 min. Mineral oil (0.2 ml) saturated with nitrogen for 30 min was added to the surface of the HEPES buffer in the anaerobic chamber, 1.2 ml HEPES buffer was drained with a syringe, and the culture was immediately observed via microscopy.

RNA Extraction and Reverse Transcription-Polymerase Chain Reaction

Total RNA from tissues and cultures was isolated by using Trizol reagent according to the manufacturer's protocol (Invitrogen Life Technology, Carlsbad, CA). Total RNA (2 μg) was used to perform reverse transcription with M-MLV transcriptase (Promega, Madison, WI) and random primers

TABLE I. Forward and Reverse Primers Used for PCR

	Forward primers	Reverse primers	Cycles	Annealing temperature (°C)
Importin-β	5′-TGGAAGTGTTGGGTGGTGAA-3′	5′-CACCAATGGCAAGAGCAATATC-3′	28	58
Transportin-1	5′-GCTCTCGATGTTCTCGCAAAT-3′	5′-GGAACGCACAAGAGCCTTTT-3′	28	58
Transportin-2	5′-TCCTCGTGAATGGGATGAAGT-3′	5′-CAGATTCCAGTCCGACAAAGC-3′	28	58
Transportin-3	5′-ATAAGCACCGAGCCGACAAT-3′	5′-GCTGAAAGGTGGGAATGCAT-3′	28	58
Importin-4	5′-TCTTTGGGTTGGGCGTACTG-3′	5′-TGAGCCACTCCTCCATGTCTT-3′	28	58
Importin-5	5′-CTTGGTGGAAAGCTCGTTCTG-3′	5′-ATTTGACCCACAGCATTGCA-3′	28	58
Importin-7	5′-CAGCTTACTACGTGCATCCATCA-3′	5′-GAGGACAGACTGGTCGGATTG-3′	28	58
Importin-8	5′-GCACAAGCCAAGGAGCACAT-3′	5′-GGCCATGACAGTTTTGTCTTCA-3′	28	58
Importin-9	5′-AAGTCCTGGGCTTTGAGAACCT-3′	5′-CTTGAGCGGCAATCCTAACAG-3′	28	58
Importin-11	5′-AGTGGGAGACACAGCCAGGTT-3′	5′-TCTGGGTCGCAATCTGGTTT-3′	28	58
Importin-13	5′-ATCCCACGGATCAGCATCAG-3′	5′-GCTACAATGTTGGCAGCATAGG-3′	28	58
Exportin-1	5′-AGCACTCATGGAGGCTCTTCA-3′	5′-GCCATGCGACTAACCATCAA-3′	28	58
Exportin-2	5′-CTTGTCTTGGATGCCTTTGCTT-3′	5′-ATCCAGTGTCAGGAGGGTATGAA-3′	28	58
Exportin-t	5′-GCAGCTCATCAGGGAGACACT-3′	5′-GAATCGATGGCCATGAGGAT-3′	28	58
Exportin-4	5′-CACAGCATTTGGAGCGGATA-3′	5′-CTGCACTGGACTGGACAGGAA-3′	28	58
Exportin-5	5′-GTGAAAGCGGTGACGGTCAT-3′	5′-GACCTTCTCCAATCGGGACAT-3′	28	58
Exportin-6	5′-GTGCGGCCTGTCTTTCTGAT-3′	5′-TGTCACCAAGTGGCACCTTTC-3′	28	58
Exportin-7	5′-CCCTGATTGCCTGAGCAAGT-3′	5′-CAGCCCAGCTTTGTGATCCT-3′	28	58
LKB1	5′-AATGGAGAGGCCAACGTCAA-3′	5′-CTGGCGGAAGTACCCATGAG-3′	26	58
GAPDH	5′-TGATGACATCAAGAAGGTGGTGAAG-3′	5′-TCCTTGGAGGCCATGTAGGCCAT-3′	24	58

(Promega) in a total volume of 25 μl. cDNA was amplified by polymerase chain reaction (PCR). Forward and reverse primers used for PCR were designed in Primer Premier 6.0. Suitable annealing temperatures (Supp. Info. Fig. 1) and cycle numbers (Supp. Info. Fig. 2) for each primer pair used in the reverse transcription-PCRs (RT-PCRs) were experimentally determined (Table I). Glyceraldehyde-3-phosphate dehydrogenase (GAPDH) was used as an internal control. The amplified products were observed with agarose gel electrophoresis. Two-percent agarose gels were prepared with the boiling method, and the ExRed dye (Zomanbio, China) was added to the gel solution before electrophoresis. After undergoing electrophoresis at 120 V for 25 min, the gels were observed with UV light in an EC3 300 Imaging System (UVP, Upland, CA). Supporting Information Figure 3A–C shows that the intensity of the bands changed in relation to the amount of starting cDNA concentrations. The intensity of the bands was quantified in Quantity One software (Bio-Rad, Hercules, CA) and perfectly represented the initial cDNA concentrations (Supp. Info. Fig. 3D,E).

Protein Extraction and Western Blot Analysis

Total protein of ischemia-treated astrocytes was extracted according to our previously published procedure (Chen et al., 2003, 2005b; Chai et al., 2013). Briefly, astrocytes were placed on ice, washed three times with ice-cold PBS, and lysed in ice-cold RIPA buffer (50 mM Tris, pH 7.5, 250 mM NaCl, 10 mM EDTA, 0.5% NP-40, 1 μg/ml leupeptin, 1 mM phenylmethylsulfonyl fluoride [PMSF], and 4 mM NaF). The cell lysate was centrifuged at 12,000*g* for 10 min at 4°C to yield the total protein extract in the supernatants.

The subcellular fractions were prepared according to a previously published procedure (Chai et al., 2013). Confluent astrocytes were washed three times with ice-cold PBS, and then 200 μl of ice-cold fractionation buffer (0.25 M sucrose, 25 mM KCl, 10 mM $MgCl_2$, 20 mM HEPES, pH 7.4, 1 mM dithiothreitol, and 0.1 mM PMSF) was added to the 35-mm culture dishes, and the cell lysate was collected in a 1.5-ml Eppendorf (Hamburg, Germany) tube on ice. The lysate was then passed through a 25-G needle 10 times with a 1-ml syringe and incubated on ice for 15 min. Centrifugation at 720*g* at 4°C for 5 min produced the crude nuclear pellet. The supernatant was transferred into a fresh tube and then centrifuged again at 1,000*g* at 4°C for 10 min; the resulting supernatant contained the cytoplasmic fraction. The crude nuclear pellet was washed by adding another 200 μl of fractionation buffer, dispersed with a pipette, passed through a 25-G needle 10 times, and centrifuged at 1,000*g* at 4°C for 10 min; the resulting pellet contained the nuclear fraction.

The protein content of the supernatant was determined by Lowry's method (Lowry et al., 1951), with slight modification, and stored at −80°C until use. Standard Western blotting analysis was performed. Samples were separated on an 8% sodium dodecyl sulfate polyacrylamide gel, and proteins were transferred onto a polyvinylidene fluoride membrane (Millipore, Billerica, MA). Exportin-7 was detected with exportin-7 polyclonal antibody (1:1,000; Santa Cruz Biotechnology, Santa Cruz, CA) and anti-rabbit IgG horseradish peroxidase conjugated antibody (1:1,000; Beijing Zhongshan Biotechnology, China). LKB1 was detected with LKB1 polyclonal antibody (1:800; Santa Cruz Biotechnology) and anti-goat IgG horseradish peroxidase (1:1,000; Santa Cruz Biotechnology). β-Actin, β-tubulin, and lamin A were used as internal controls to quantify equal loadings.

Immunofluorescence Staining and Microscopy

Immunofluorescence staining and microscopy were performed as previously described (Chai et al., 2013). Cells on culture dishes were washed with ice-cold PBS three times, fixed with 4% paraformaldehyde for 10 min, washed with ice-cold

PBS three times for 5 min each, permeabilized with 0.3% Triton X-100 for 30 min, and washed with PBS three times for 5 min each. After blocking of nonspecific binding with 3% bovine serum albumin in PBS for 1 hr at room temperature, the cells were incubated with primary antibodies rabbit anti-exportin-7 antibody (1:100; Santa Cruz Biotechnology) and goat anti-LKB1 antibody (1:100; Santa Cruz Biotechnology) overnight at 4°C, washed with ice-cold PBS three times for 5 min each, incubated with Alexa Fluor 488-conjugated donkey anti-rabbit antibody (1:100; Beyotime, shanghai, China) or Cy3-conjugated donkey anti-goat antibody (1:100; Beyotime) for 1 hr, and washed with ice-cold PBS three times for 5 min each. Finally, the cells were mounted on a slide, and the stained sections were examined through an inverted FluoView FV1000 confocal microscope (Olympus, Tokyo, Japan) with a ×60 oil objective. During microscopy, lasers with wavelengths of 405, 488, and 549 were selected to stimulate the fluorescence separately. The pinhole used was 100 μs, and the optical slice thickness was 0.64 μm. Photographs were processed in FluoView FV1000 software (Olympus) without deconvolution and arranged in Photoshop CS15 (Adobe Systems, San Jose, CA).

Plasmid Construction and Transient Transfection

The coding regions of the mouse LKB1 gene without the stop codon was isolated from primary cultures of astrocytes and inserted into the pDsRed-N1 vector (LKB1-DsRed; Clontech, Mountain View, CA). The construct was confirmed by DNA sequencing.

Plasmids were transiently transfected into confluent primary astrocyte cultures with Lipofectamine2000 reagent (Invitrogen) with serum-free DMEM, and the culture medium was replaced with medium containing 10% FBS after 6 hr. Ischemia treatment was performed 24 hr after transfection.

Fluorescence Recovery After Photobleaching Assay

Astrocytes were transfected with LKB1-DsRed or pDsRed-N1 plasmid. After 24 hr, the medium was replaced with HEPES buffer, and the cells were imaged at room temperature via confocal microscopy. Photobleaching was performed mainly as described by Dorfman and Macara (2008). Regions of interest were photobleached with the 549-nm laser line at 100% intensity, and then the images were observed at 15% intensity at 5, 30, 60, 150, 300, and 600 sec after bleaching.

Statistical Analysis

All experiments were performed at least three times with cultures from at least two different batches. Results were analyzed in Prism 5.0 (GraphPad Software, La Jolla, CA), and statistical analysis was performed by Student's *t*-test or by one-way ANOVA, with Tukey's multiple-comparisons test. Results are expressed as mean ± SEM. $P < 0.05$ was considered significant.

RESULTS

Importin mRNA Expression in the CNS

The mRNA levels of all 11 importins (importin-β; transportin-1, -2, and -3; and importin-4, -5, -7, -8, -9, -11, and -13) were measured with RT-PCR (Fig. 1). mRNA expression of the 11 importins was detected in the cerebral cortex, cerebellum, hippocampus, and brainstem of adult mice (Fig. 1A). The 11 importin mRNAs were also detected in primary cultures of neurons and astrocytes (Fig. 1A). For each importin, its expression level was similar in the different brain tissues (Fig. 1B). However, all of the importins had higher expression levels in primary cultures of neurons than in primary cultures of astrocytes, except for importin-3 and importin-13 (Fig. 1C).

Exportin mRNA Expression in the CNS

The mRNA levels of all seven exportins (exportin-1, -2, -t, -4, -5, -6, and -7) were measured with RT-PCR (Fig. 2). All seven exportin mRNAs were detected in the cerebral cortex, cerebellum, hippocampus, and brainstem of adult mice and in primary cultures of neurons and astrocytes. Exportin-4, exportin-5, and exportin-7 were differentially expressed in tissues collected from different parts of the brain (Fig. 2B). All seven exportins were expressed at higher levels in primary cultures of neurons than in primary cultures of astrocytes (Fig. 2C). We also compared the expression levels of exportin-7 in different brain tissues and in primary cultures of astrocytes and neurons with both RT-PCR and real-time PCR (Supp. Info. Fig. 4). Both RT-PCR and real-time PCR results showed that exportin-7 expression levels were different in different brain tissues. Among the different brain structures, exportin-7 had the highest expression levels in the hippocampus, whereas the lowest expression levels were measured in the brainstem. In primary cultures of astrocytes and neurons, exportin-7 expression levels were higher in neurons than in astrocytes.

Importin mRNA Expression in Astrocytes Under Ischemia

Importin expression levels in astrocytes during ischemia for 0.5–6 hr were studied with RT-PCR (Fig. 3). Both importin-4 ($P < 0.01$) and importin-5 ($P < 0.05$) increased significantly after ischemia treatment for 1 hr, whereas importin-7 decreased significantly after ischemia for 0.5 hr ($P < 0.05$). At the same time, the expression of importin-8 decreased significantly after ischemia treatment for 4 hr ($P < 0.001$), whereas the expressions of most other importins (importin-β, -4, -7, -8, and -13 and transportin-1, -2, and -3) decreased significantly after ischemia treatment for 6 hr (importins, $P < 0.05$, $P < 0.01$, $P < 0.001$, $P < 0.001$, $P < 0.05$, respectively; transportins, $P < 0.01$, $P < 0.001$, $P < 0.01$, respectively).

Exportin mRNA Expression in Astrocytes Under Ischemia

We also measured the expression levels of exportins in astrocytes under ischemia from 0.5–6 hr with RT-PCR (Fig. 4). Decreased mRNA expressions of exportin-1 ($P < 0.05$) and exportin-4 ($P < 0.01$) were observed after ischemia treatment for 6 hr. We noted that, among all the

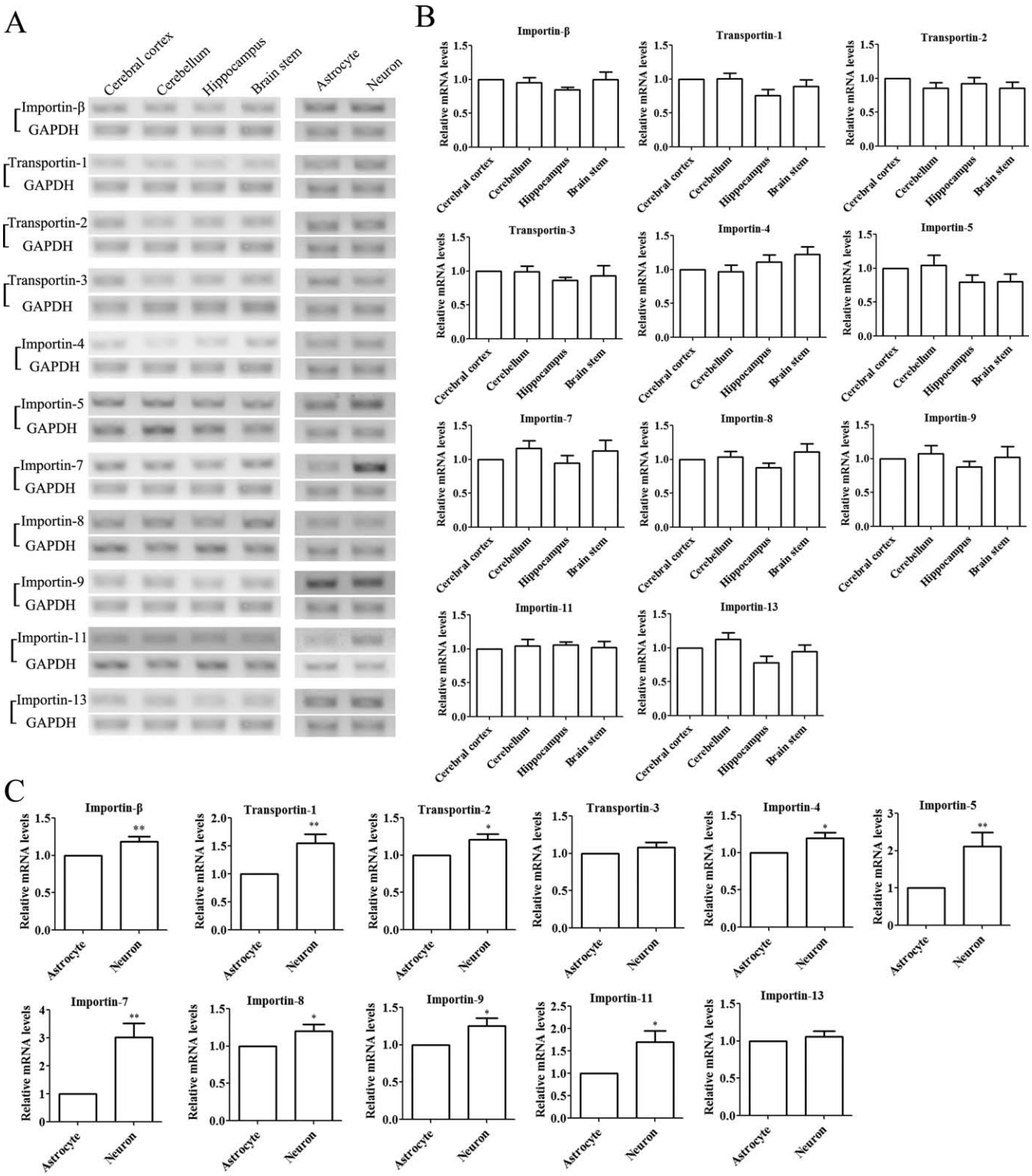

Fig. 1. Expression of importins in the mouse brain and primary cultures of astrocytes and neurons. **A:** Representative RT-PCR results reveal the expressions of 11 types of importins (importin-β; transportin-1, -2, and -3; and importin-4, -5, -7, -8, -9, -11, and -13) in tissues of the cerebral cortex, cerebellum, hippocampus, and brainstem of 9-week-old male mice; in primary astrocyte cultures; and in primary neuron cultures. **B,C:** Statistical data for the PCR results from A. The ratios of the relative expression levels of importins (the ratio of the expression levels of importins to the expression level of the internal control GAPDH) to that of importins in the cerebral cortex or in astrocytes are presented in the final graphic. GAPDH was amplified simultaneously as an internal control. N = 9. $^{\star}P < 0.05$, $^{\star\star}P < 0.01$.

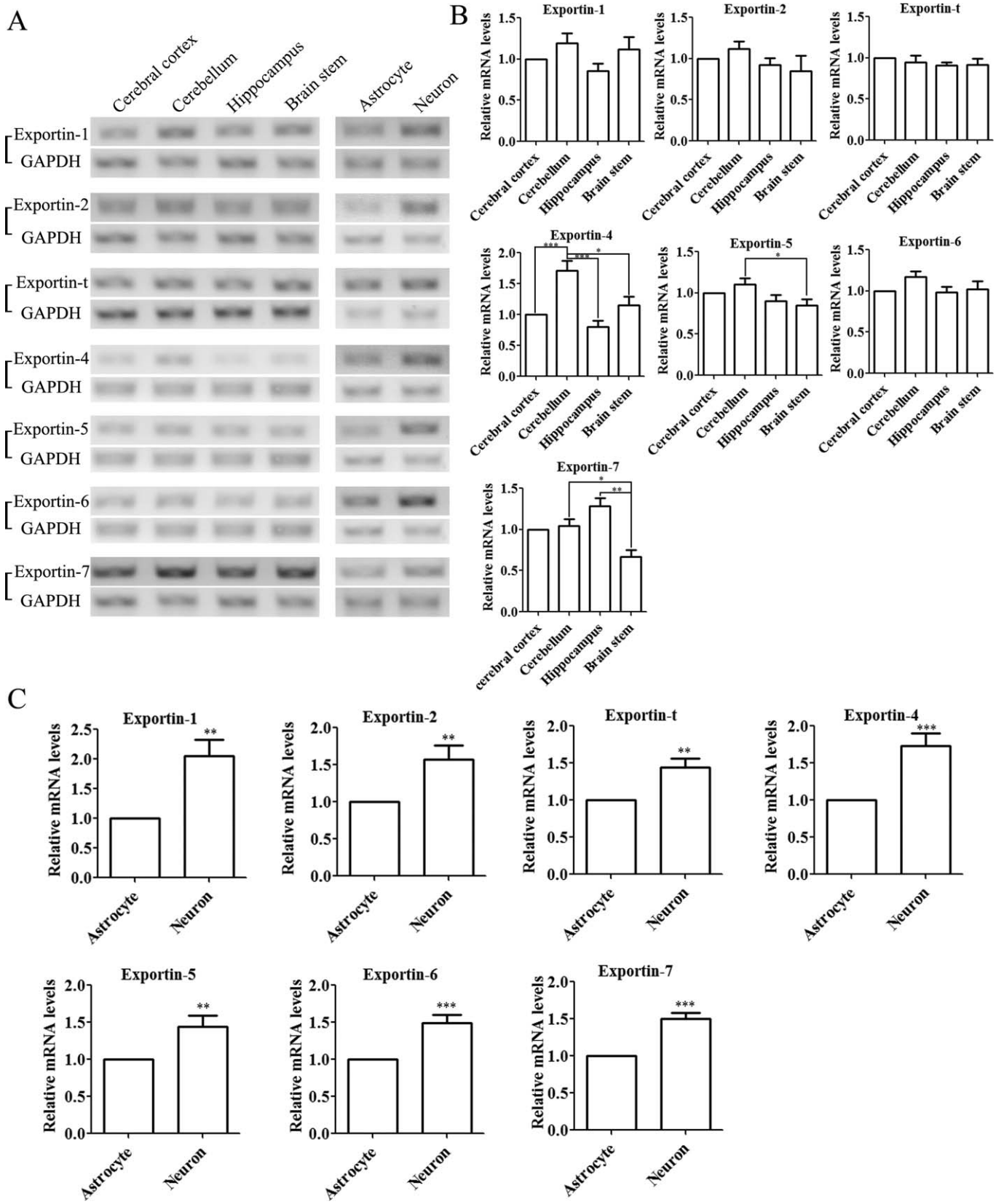

Fig. 2. Expression of exportins in mouse brain and primary cultures of astrocytes and neurons. **A:** Representative RT-PCR results reveal the expression of seven types of exportins (exportin-1, -2, -t, -4, -5, -6, and -7) in tissues of the cerebral cortex, cerebellum, hippocampus, and brainstem of 9-week-old male mice; in primary astrocyte cultures; and in primary neuron cultures. **B,C:** Statistical data for the PCR results from A. The ratios of the relative expression levels of exportins (the ratio of the expression levels of exportins to the expression level of internal control) to that of exportins in the cerebral cortex or in astrocytes are presented in the final graphic. GAPDH was amplified simultaneously as an internal control. N = 9. $\star P < 0.05$, $\star\star P < 0.01$, $\star\star\star P < 0.001$.

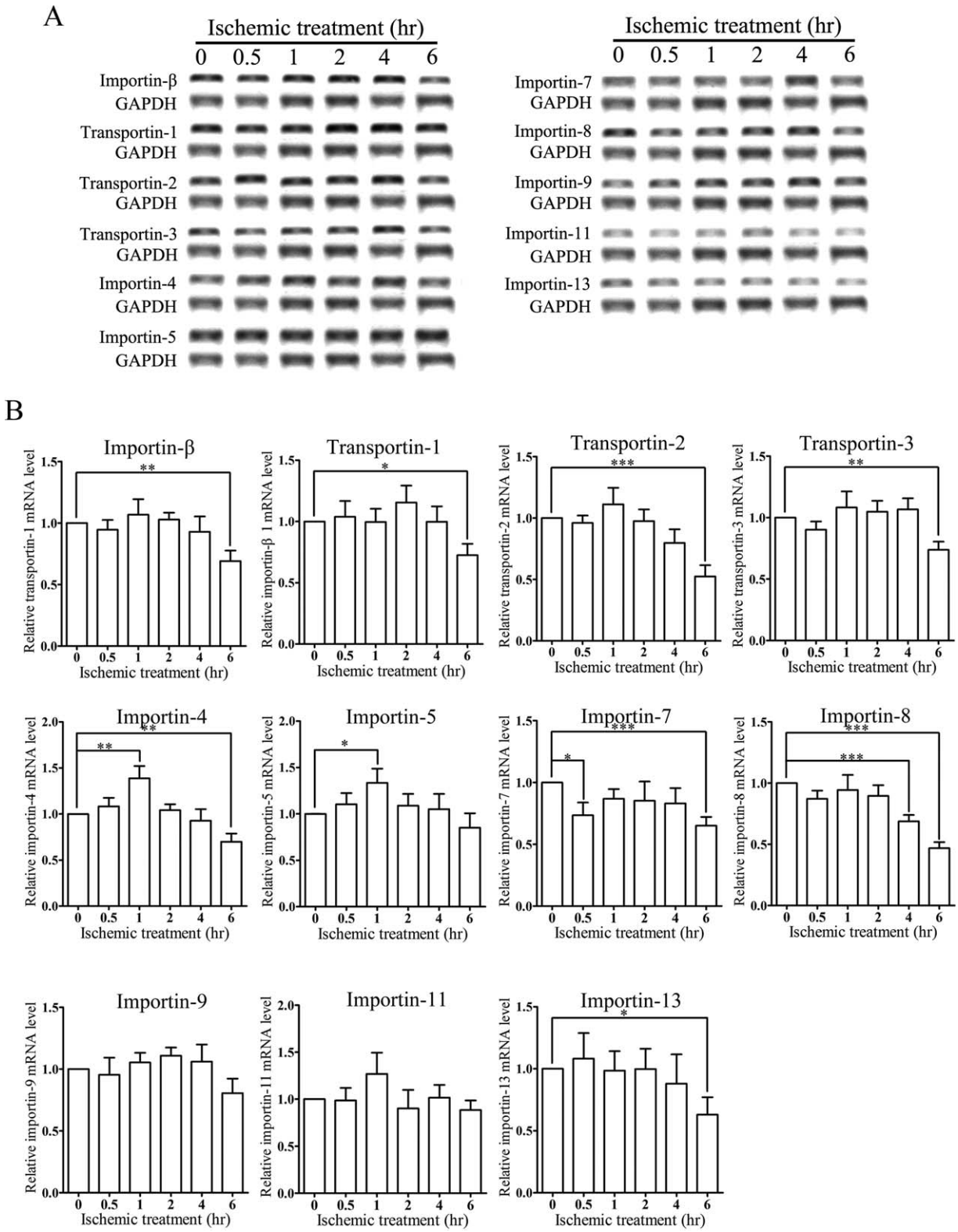

Fig. 3. mRNA expression of importins in astrocytes under ischemia. **A,B:** Representative RT-PCR results (A) and statistical results (B) reveal the expression changes of importins in primary cultures of astrocytes under ischemia treatment for different lengths of time (0.5–6 hr). GAPDH was amplified simultaneously as an internal control. Quantitative data were analyzed by one-way ANOVA and Tukey's multiple-comparisons test. $N = 7$. $^{\star}P < 0.05$, $^{\star\star}P < 0.01$, $^{\star\star\star}P < 0.001$.

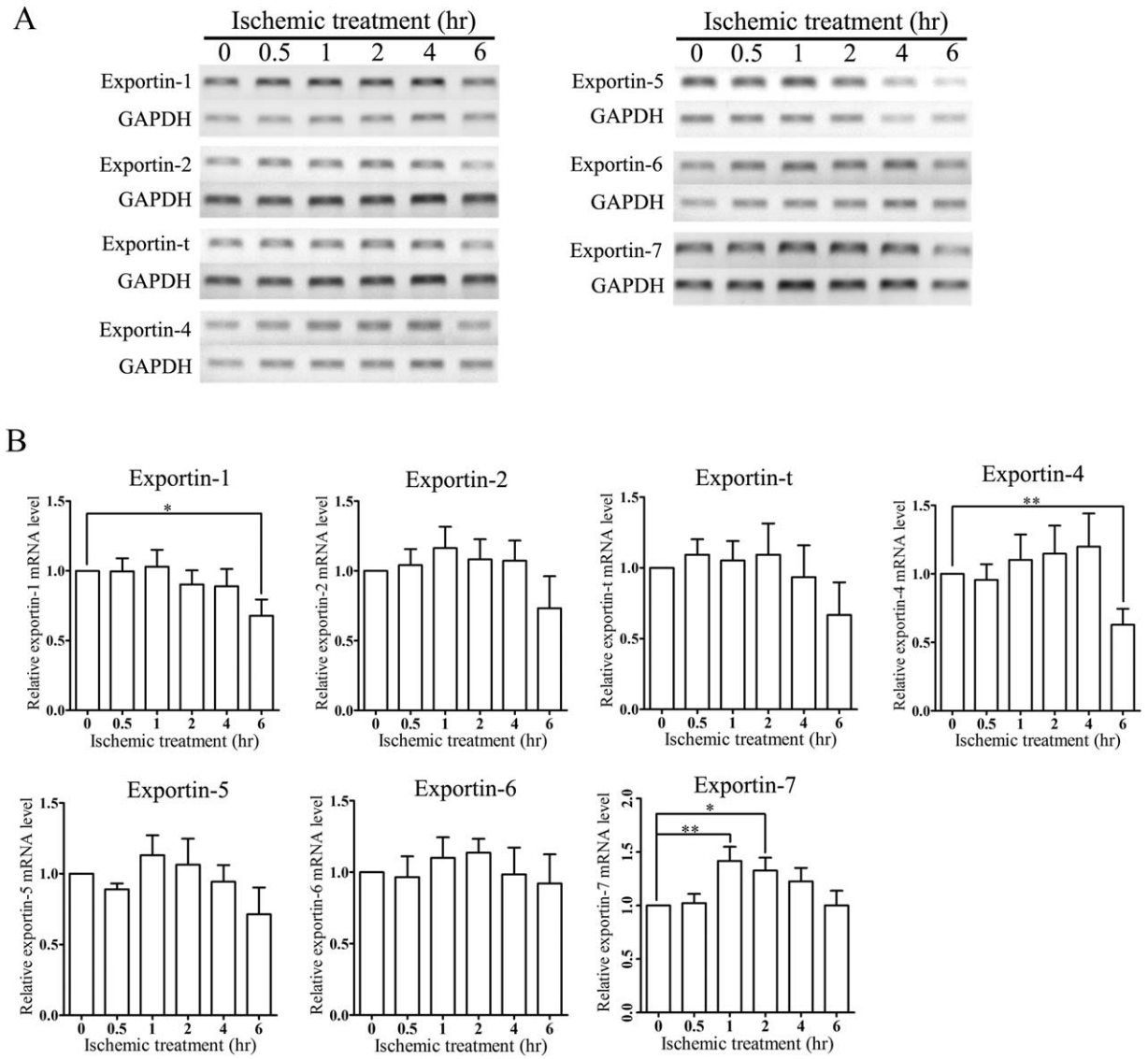

Fig. 4. mRNA expression of exportins in astrocytes under ischemia. **A,B:** Expression of exportins varied in astrocytes under ischemia. Representative RT-PCR results (A) and statistical results (B) reveal the mRNA expression changes of exportins in primary cultures of astrocytes under ischemia treatment for different lengths of time (0.5–6 hr). GAPDH was amplified simultaneously as an internal control. Quantitative data were analyzed by one-way ANOVA and Tukey's multiple-comparisons test. N = 7. $\star P < 0.05$, $\star\star P < 0.01$.

exportins, only exportin-7 mRNA expression increased significantly after ischemia treatment for 1 hr ($P < 0.01$) and 2 hr ($P < 0.05$). The other exportins did not show any significant variance in astrocytes under ischemia during the period of study.

Protein Expression and Localization Changes of Exportin-7 in Astrocytes Under Ischemia

Subcellular localization of exportin-7 in primary cultures of astrocytes was also observed with immunostaining (Fig. 5A). The laser confocal scanning microscopy images showed that intrinsic exportin-7 was distributed both in the nucleus and in the cytoplasm of astrocytes, with a higher aggregation around the nucleus. To confirm that the upregulation of exportin-7 mRNA caused an increase in protein, we performed Western blotting to explore exportin-7 protein expression changes after ischemia (Fig. 5B). The exportin-7 protein was increased in astrocytes after ischemia treatment for 1 and 2 hr ($P < 0.001$).

We also observed the expression and distribution changes of exportin-7 under ischemia treatment with immunostaining (Figs. 5C, 9). In the confocal laser microscopy images there was no significant difference between the exportin-7 signals in the cytoplasm and in the nucleoplasm of astrocytes without ischemia. During ischemia treatment for 0–4 hr we noticed that the exportin-7 signal intensity increased inside the nuclei of astrocytes after 1 hr, whereas with longer ischemia

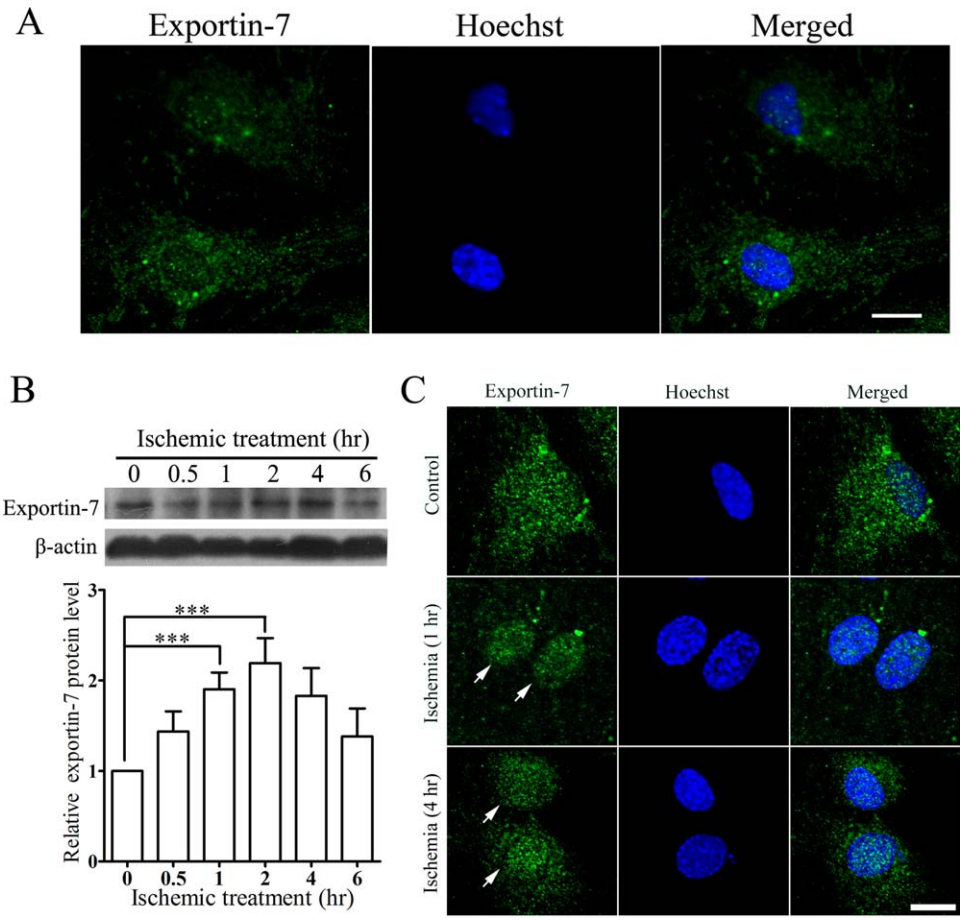

Fig. 5. Protein expression changes of exportin-7 in astrocytes under ischemia. **A:** Localization of exportin-7 in astrocytes under normal conditions. Primary astrocyte cultures were subjected to immunofluorescence staining of exportin-7 and observed via laser confocal scanning microscopy. Representative images show the intrinsic exportin-7 (green) localization in astrocytes; nuclei were stained with Hoechst (blue). **B:** Protein expression changes of exportin-7 in astrocytes under ischemia. Representative Western blotting results and statistical results reveal the protein expression changes of exportin-7 in astrocytes under ischemia for 0–6 hr. β-Actin was detected simultaneously as an internal control. Quantitative data were analyzed by one-way ANOVA and Tukey's multiple-comparison test. N = 7. ***$P < 0.001$. **C:** Exportin-7 distribution changes in astrocytes under ischemia. Primary astrocyte cultures after 0, 1, and 4 hr ischemia treatment were subjected to immunofluorescence staining of exportin-7 and observed via laser confocal scanning microscopy. Representative images reveal the exportin-7 (green, arrows) distribution changes in astrocytes under ischemia; nuclei were stained with Hoechst (blue). Scale bars = 10 μm. [Color figure can be viewed in the online issue, which is available at wileyonlinelibrary.com.]

treatment (2–4 hr) the exportin-7 signal intensity inside the nuclei gradually decreased.

Expression and Distribution Changes of LKB1 in Astrocytes After Ischemia Treatment

After confirming that both mRNA and protein levels of exportin-7 were increased by ischemia, we examined whether this increase would lead to changes in the expression and distribution of the exportin-7 substrate LKB1 (Fig. 6). RT-PCR of LKB1 mRNA levels in astrocytes after ischemia treatment for 0.5–6 hr (Fig. 6A) revealed that LKB1 mRNA did not change under ischemia treatment. However, LKB1 protein levels increased significantly in astrocytes after ischemia treatment for 1 and 2 hr (Fig. 6B), indicating that LKB1 protein expression responded to ischemia injury in astrocytes. Examination of LKB1 protein expression changes in the nucleus and in the cytoplasm of astrocytes by Western blotting (Fig. 6C; Supp. Info. Fig. 5) revealed that the ratio of cytoplasmic LKB1 to nuclear LKB1 increased significantly in astrocytes after ischemia treatment for 0.5–2 hr, indicating an increased LKB1 translocation from the nucleus into the cytoplasm. The increased translocation of LKB1 from the nucleus to the cytoplasm in astrocytes under ischemia treatment was also confirmed by immunostaining and LKB1-DsRed transfection (Fig. 6D; see also Fig. 8).

Transport of LKB1-DsRed From the Cytoplasm Into the Nucleus in Astrocytes

To confirm that LKB1 could be transported into the nucleus after synthesis in astrocytes, we studied the transport of LKB1-DsRed from the cytoplasm into the nucleus

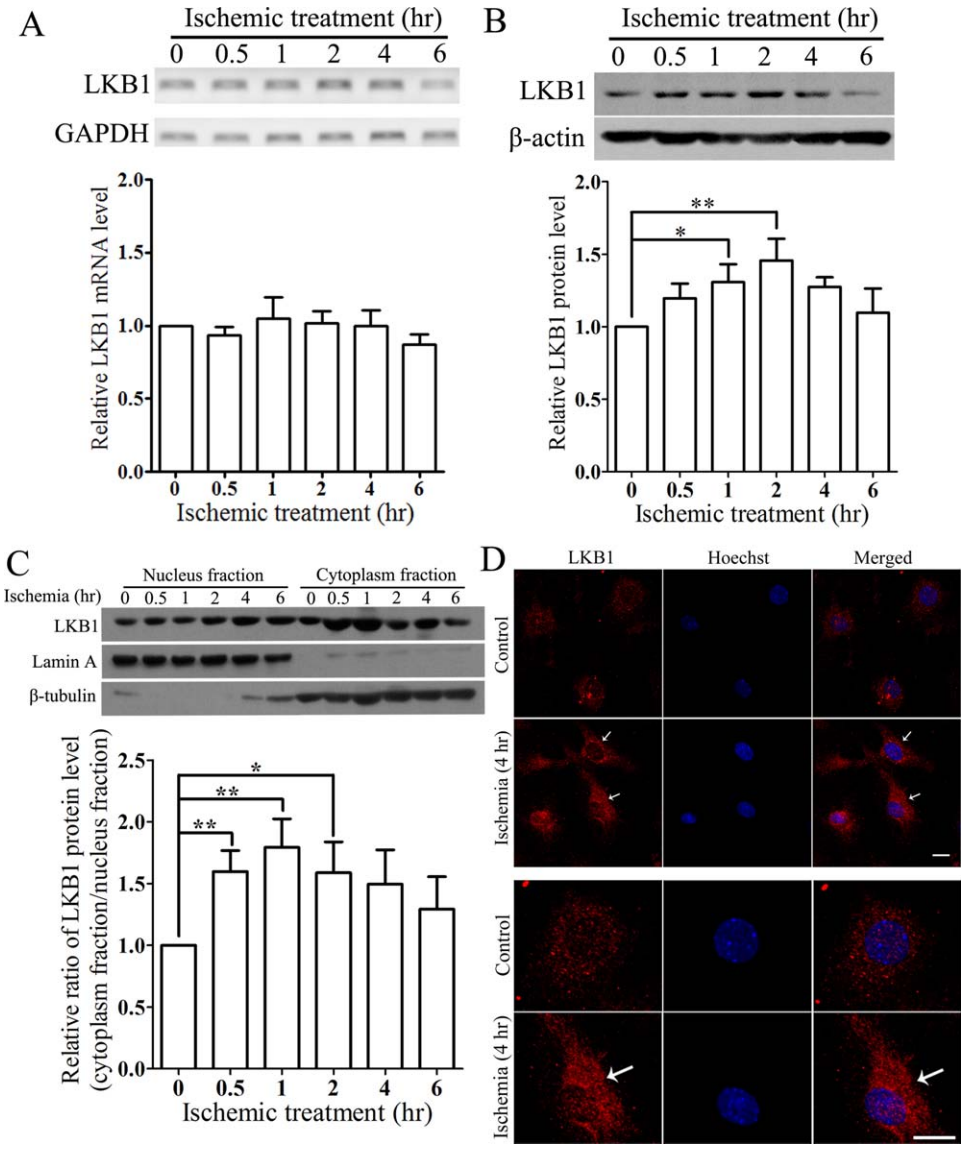

Fig. 6. Expression and translocation of LKB1 in astrocytes under ischemia. **A:** LKB1 mRNA expression in astrocytes under ischemia. Representative RT-PCR results and statistical results reveal mRNA levels of LKB1 in astrocytes under ischemia for 0–6 hr. GAPDH was amplified simultaneously as an internal control. Quantitative data were analyzed by one-way ANOVA and Tukey's multiple-comparisons test. N = 7. **B:** Protein expression of LKB1 in astrocytes under ischemia. Representative Western blotting results and statistical results reveal the protein expression changes of LKB1 in astrocytes under ischemia for 0–6 hr. β-Actin was detected simultaneously as an internal control. Quantitative data were analyzed by one-way ANOVA and Tukey's multiple-comparisons test. N = 7. $\star P < 0.05$, $\star\star P < 0.01$. **C:** Subcellular expression changes of LKB1 protein in astrocytes under ischemia. Representative Western blotting results and statistical results reveal the ratio of relative LKB1 protein levels in the cytoplasm to those in the nucleus in astrocytes under ischemia for 0–6 hr. Lamin A and β-tubulin were detected as internal controls for calculating relative LKB1 levels in the nuclear fraction and in the cytoplasm fraction, respectively. Quantitative data were analyzed by one-way ANOVA and Tukey's multiple-comparisons test. N = 7. $\star P < 0.05$, $\star\star P < 0.01$. **D:** LKB1 expression and distribution changes in astrocytes after ischemia. Primary astrocyte cultures after 0 and 4 hr of ischemia were subjected to immunostaining with LKB1 antibody and then observed via laser confocal scanning microscopy. Representative images reveal LKB1 (red, arrows) expression and distribution changes in astrocytes; nuclei were stained with Hoechst (blue). Images in the lower panels show the expression and distribution changes of LKB1 in astrocytes under ischemia treatment at higher magnification. Scale bars = 10 μm. [Color figure can be viewed in the online issue, which is available at wileyonlinelibrary.com.]

with a fluorescence recovery after photobleaching (FRAP) assay (Fig. 7). In the confocal laser microscopy images, LKB1-DsRed signals in the nuclei of astrocytes, both without ischemia injury and with ischemia injury for 30 min, could recover after photobleaching (Fig. 7A,B). However, the recovery of the LKB1-DsRed signal in the nuclei of astrocytes without ischemia injury was much faster than that in the nuclei of astrocytes with ischemia injury

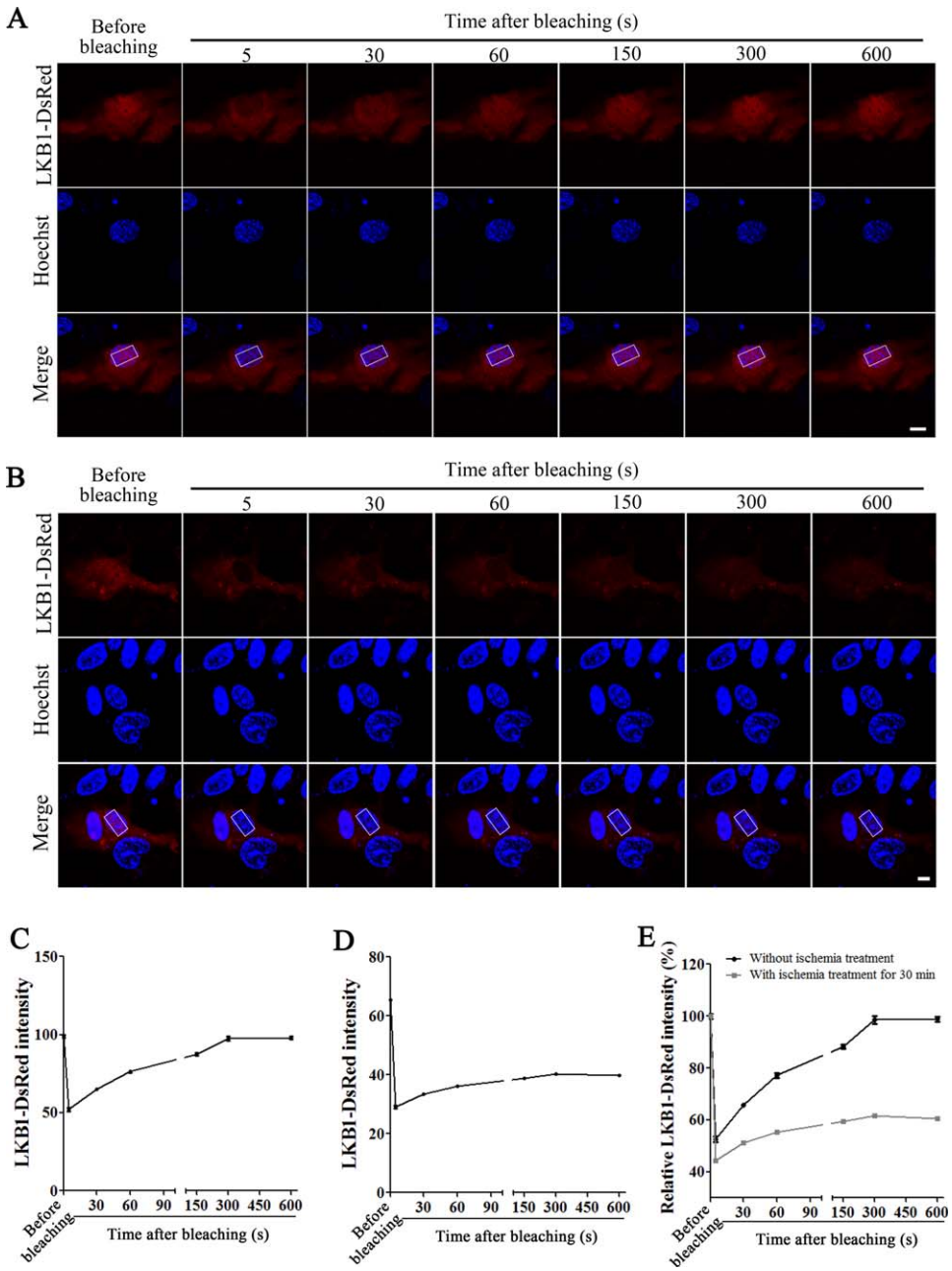

Fig. 7. Transport of LKB1-DsRed from the cytoplasm to the nuclei of astrocytes. **A,B:** LKB1-DsRed signals (red) in nuclei of astrocytes without (A) or with (B) ischemia treatment for 30 min are shown before bleaching and at different times (5–600 sec) after bleaching via laser confocal scanning microscopy; nuclei were stained with Hoechst (blue). **C,D:** Quantification data show LKB1-DsRed signal intensity changes in the boxes from A (C) and from B (D) before bleaching and at different times (5–600 sec) after bleaching. **E:** Quantification data show the relative LKB1-DsRed intensity (normalized to the LKB1-DsRed signal before bleaching) of the boxes from A (C) and from B (D) before bleaching and at different times (5–600 sec) after bleaching. Scale bars = 10 μm. [Color figure can be viewed in the online issue, which is available at wileyonlinelibrary.com.]

(Fig. 7C–E). The LKB1-DsRed signal in the nuclei of astrocytes without ischemia recovered to 100% of the intensity before photobleaching within 300 sec, whereas the LKB1-DsRed signal in the nuclei of astrocytes under ischemia treatment for 30 min recovered only to 60% of the intensity before photobleaching after 600 sec (Fig. 7E). We also observed distribution changes of pDsRed-N1 in astrocytes with FRAP, and the confocal laser microscopy images showed that the DsRed signal had not recovered 600 sec after bleaching (Supp. Info. Fig. 6).

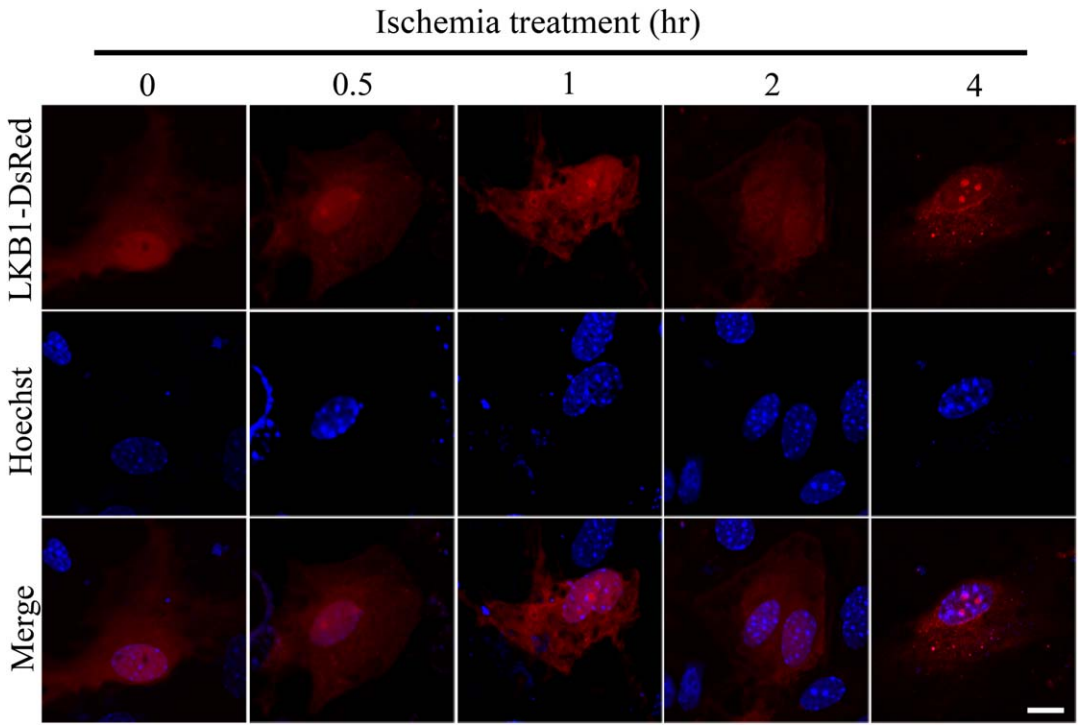

Fig. 8. Distribution changes of LKB1-DsRed in astrocytes under ischemia. After astrocytes had been transfected for 24 hr, the LKB1-DsRed (red) signals in astrocytes under ischemia (0–6 hr) were observed via laser confocal scanning microscopy; nuclei were stained with Hoechst (blue). Scale bar = 10 μm. [Color figure can be viewed in the online issue, which is available at wileyonlinelibrary.com.]

Distribution Changes of LKB1-DsRed in Astrocytes Under Ischemia

To observe the distribution changes of LKB1 in astrocytes under ischemia more clearly, we also observed the LKB1-DsRed distribution in astrocytes under ischemia from 0 to 6 hr via a confocal laser microscope (Fig. 8). In astrocytes without ischemia, the LKB1-DsRed signal was much higher in the nucleus than in the cytoplasm. During the ischemia treatment from 0.5 to 2 hr, the intensity of the LKB1-DsRed signal in the nucleus gradually became similar to that in the cytoplasm, whereas the intensity of the LKB1-DsRed signal in the nucleus was lower than that in the cytoplasm after ischemia for 4 hr.

Colocalization Changes of LKB1 and Exportin-7 in Astrocytes After Ischemia Treatment

To determine whether exportin-7 plays a role in the distribution changes of LKB1 in astrocytes under ischemia, we also studied colocalization changes of LKB1 and exportin-7 in astrocytes after ischemia treatment with double immunostaining (Fig. 9). In the confocal laser microscopy images of astrocytes without ischemia, the staining of LKB1 was too faint to show any possible colocalized distribution of LKB1 and exportin-7. After ischemia treatment for 1–4 hr, the expression of LKB1 was obviously increased, and the colocalized distribution of LKB1 and exportin-7 was observed accompanying the distribution changes of exportin-7 and LKB1 (Fig. 9A,B).

DISCUSSION

This study demonstrates that all 11 importin and all seven exportin mRNAs are differently expressed in the cerebral cortex, cerebellum, hippocampus, and brainstem and in primary cultures of astrocytes and neurons. This finding is consistent with the expression patterns of importin-β; transportin-1, -2, and -3; and importin-9 and -13 in the brain that have been previously reported (Kortvely et al., 2005; Hosokawa et al., 2008; Sato et al., 2011; You et al., 2013). Moreover, this study presents comprehensive information on the expression of all of the importins and exportins in some major structures of the brain in adult mice. The functions of importins and exportins in a cell or an organ are highly dependent on the amount present (Hosokawa et al., 2008; You et al., 2013), and our findings provide new evidence demonstrating the variations in importins and exportins in different brain structures and cell types. Further experimentation is required to determine how these differences affect transport mechanisms and whether they have any physiological or pathological significance.

We examined the mRNA levels of the importins and exportins in astrocytes after ischemia treatment for 0–6 hr. We observed that the mRNA levels of importin-β; transportin-1, -2, and -3; importin-4, -5, -7, -8, and -13; and exportin-1 and -4 were significantly decreased in astrocytes after ischemia treatment for 6 hr. Because most astrocytes die after 6 hr of in vitro ischemia (Yu et al.,

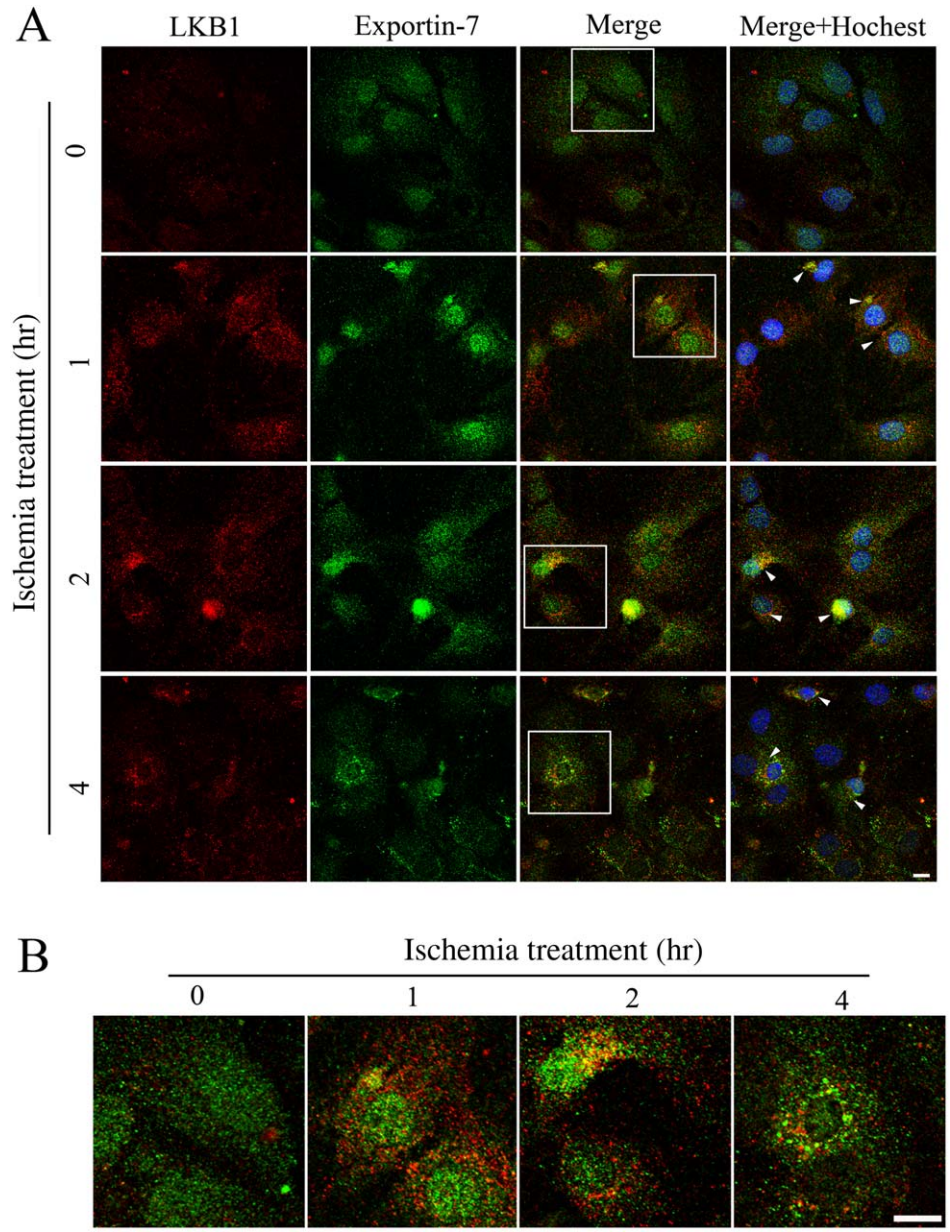

Fig. 9. Expression and distribution of LKB1 and exportin-7 in astrocytes under ischemia. **A,B:** LKB1 and exportin-7 expression and distribution changes in astrocytes after ischemia. Primary astrocyte cultures, after 0–4 hr of ischemia, were subjected to immunostaining with LKB1 and exportin-7 antibodies and then observed via laser confocal scanning microscopy. Representative images reveal LKB1 (red) and exportin-7 (green) expression and distribution changes in astrocytes; nuclei were stained with Hoechst (blue). Colocalization of LKB1 and exportin-7 are indicated by arrowheads. The boxed areas in A are shown at higher magnification in B. Scale bar = 10 μm. [Color figure can be viewed in the online issue, which is available at wileyonlinelibrary.com.]

2001), the decreased expression of these importins and exportins might be related to the low viability of the cells during ischemia treatment. The mRNA expressions of importin-4 and -5 and exportin-7 were significantly increased after ischemia treatment for 1 hr. We did not study exportin-7 expression in ischemic neurons because the neuronal response to ischemia is very different from that of astrocytes, with the response and cell death occurring very rapidly. This creates difficulties in recording and measuring the details of changes from the initiating injury to the end result, cell death. Proper expression and regulation of importins and exportins is critical for the normal function and the dysfunction of the nucleocytoplasmic transport machinery. Decreased importin-β levels are associated with the pathogenesis of ALS (Nagara et al., 2013), whereas increased expression of importin-α2 is correlated with higher histological grade, more proliferative activity, and poorer prognosis in patients with

infiltrative astrocytomas (Gousias et al., 2012). The upregulation of importin-4 and -5 and exportin-7 that we observed indicates that these transport receptors might be involved in astrocytic responses to ischemic insult.

We confirm that the protein level of exportin-7 is also upregulated in astrocytes under ischemia. The endogenous exportin-7 in astrocytes under normal conditions was distributed throughout the cell, with a slight aggregation around the nuclear envelope, consistent with the distribution reported for HeLa cells (Koch et al., 2000; Kutay et al., 2000). We also observed that exportin-7 significantly aggregated inside the nucleus after 1 hr of ischemia, and exportin-7 expression increased both inside and around the nuclei of astrocytes after 4 hr of ischemia. These data suggest that exportin-7 is involved in a more intensive transport process during ischemia.

As previously discussed, exportin-7 is involved in the nuclear export of LKB1, a kinase with multiple functions in cells, including energy metabolism regulation (Shaw et al., 2005; Dorfman and Macara, 2008; Courchet et al., 2013). We also observed that the protein ratio of LKB1 in the cytoplasm to that in the nucleus increased significantly in astrocytes after 0.5, 1, and 2 hr of ischemia, an indication of the translocation of LKB1 from the nucleus to the cytoplasm in astrocytes during ischemia injury. Although the elevation of this ratio might also have been caused by increased translation in the cytoplasm, the data confirmed that the elevation of LKB1 in the cytoplasm of astrocytes was more likely related to the nuclear export of LKB1. The data indicated that the elevation of the ratio occurred at 0.5 hr, whereas the total protein level of LKB1 did not increase until 1 hr. In addition, as a protein with a nuclear localization sequence, LKB1 would be transported into the nucleus after being translated in the cytoplasm, and this was confirmed by the results from the FRAP assay. From the FRAP data, we also observed a reduced transporting of LKB1-DsRed from the cytoplasm to the nucleus in astrocytes after ischemia injury; this was caused by the increased nuclear export of LKB1. Moreover, the translocation of LKB1 from the nucleus to the cytoplasm was also observed through immunostaining and LKB1-DsRed transfection. Translocation of LKB1 from the nucleus to the cytoplasm has been found to be important for its functioning (Mingot et al., 2004; Shaw et al., 2005; Dorfman and Macara, 2008). LKB1 is exported from the nucleus to the cytoplasm, and its catalytic activity toward its substrates is significantly increased tenfold (Boudeau et al., 2003). Mutants of LKB1, with disruption of the nuclear location signal, still retain the ability to suppress cell growth, suggesting that the cytoplasmic pool of LKB1 plays an important role in mediating its tumor suppressor function (Tiainen et al., 2002; Alessi et al., 2006). Previously we reported the linkage between energy stress and ischemia in astrocytes by utilizing the same in vitro ischemia model (Yu et al., 2002). The current study confirms that LKB1, an important kinase in mediating energy homeostasis in response to energy stress (Shaw et al., 2004, 2005; Ohashi et al., 2010), is also involved in ischemia in astrocytes. LKB1 has been reported to be activated following physiological and pathological stimuli, such as exercise, hypoxia, or glucose deprivation, when AMP levels increase (Hardie et al., 2003); recently, LKB1 activation was proved to be essential for neuronal cell survival under mitochondrial dysfunction (Ma et al., 2013). However, this study is the first to examine the role of LKB1 in astrocytes during ischemia.

Although LKB1 can be transported from the nucleus to the cytoplasm through exportin-1 or exportin-7 (Dorfman and Macara, 2008), the data show that the expression of exportin-1 did not change significantly in astrocytes under ischemia, suggesting a more important role for exportin-7 in the translocation of LKB1 in astrocytes, inasmuch as both the increased cytoplasmic and nuclear LKB1 ratio and the increased exportin-7 expression appeared in astrocytes during ischemia for 0.5–2 hr. The mRNA levels of LKB1 did not change significantly in astrocytes under ischemia for 0–6 hr, whereas LKB1 protein levels increased significantly in astrocytes after ischemia treatment for 2 hr, indicating that LKB1 could be upregulated in a posttranscriptional manner in astrocytes under ischemia.

In summary, this study reveals information on the expression of all of the importins and exportins in the cerebral cortex, cerebellum, hippocampus, and brainstem of adult mice as well as in cultured neurons and astrocytes. It also shows that importins and exportins display different expression changes in astrocytes under ischemia. Exportin-7 was upregulated at both mRNA and protein levels and accumulated inside and around the nucleus. LKB1, a substrate of exportin-7, showed significant nuclear export in astrocytes after a short period of ischemia, and the protein levels were upregulated after longer ischemia treatment. We have shown that exportin-7 responds to ischemia through mediating LKB1, a multifunctional kinase, and increases its translocation from the nucleus to the cytoplasm in astrocytes.

REFERENCES

Alessi DR, Sakamoto K, Bayascas JR. 2006. LKB1-dependent signaling pathways. Annu Rev Biochem 75:137–163.

Bai HY, Li AP. 2013. P2X(7) receptors in cerebral ischemia. Neurosci Bull 29:390–398.

Boudeau J, Baas AF, Deak M, Morrice NA, Kieloch A, Schutkowski M, Prescott AR, Clevers HC, Alessi DR. 2003. MO25alpha/beta interact with STRADalpha/beta enhancing their ability to bind, activate, and localize LKB1 in the cytoplasm. EMBO J 22:5102–5114.

Chai RC, Jiang JH, Kwan Wong AY, Jiang F, Gao K, Vatcher G, Hoi Yu AC. 2013. AQP5 is differentially regulated in astrocytes during metabolic and traumatic injuries. Glia 61:1748–1765.

Chen XQ, Chen JG, Zhang Y, Hsiao WW, Yu AC. 2003. 14-3-3Gamma is upregulated by in vitro ischemia and binds to protein kinase Raf in primary cultures of astrocytes. Glia 42:315–324.

Chen XQ, Fung YW, Yu AC. 2005a. Association of 14-3-3gamma and phosphorylated bad attenuates injury in ischemic astrocytes. J Cereb Blood Flow Metab 25:338–347.

Chen XQ, Lau LT, Fung YW, Yu AC. 2005b. Inactivation of bad by site-specific phosphorylation: the checkpoint for ischemic astrocytes to initiate or resist apoptosis. J Neurosci Res 79:798–808.

Chen XQ, Liu S, Qin LY, Wang CR, Fung YW, Yu AC. 2005c. Selective regulation of 14-3-3eta in primary culture of cerebral cortical neurons and astrocytes during development. J Neurosci Res 79:114–118.

Courchet J, Lewis TL Jr, Lee S, Courchet V, Liou DY, Aizawa S, Polleux F. 2013. Terminal axon branching is regulated by the LKB1-NUAK1 kinase pathway via presynaptic mitochondrial capture. Cell 153:1510–1525.

Deng L, Bosse Y, Brown N, Chin LY, Connolly SC, Fairbank NJ, King GG, Maksym GN, Pare PD, Seow CY, Stephen NL. 2009. Stress and strain in the contractile and cytoskeletal filaments of airway smooth muscle. Pulmonary Pharmacol Ther 22:407–416.

Dong Y, Liu HD, Zhao R, Yang CZ, Chen XQ, Wang XH, Lau LT, Chen J, Yu AC. 2009. Ischemia activates JNK/c-Jun/AP-1 pathway to upregulate 14-3-3gamma in astrocyte. J Neurochem 109:182–188.

Dong Y, Zhao R, Chen XQ, Yu AC. 2010. 14-3-3Gamma and neuroglobin are new intrinsic protective factors for cerebral ischemia. Mol Neurobiol 41:218–231.

Dorfman J, Macara IG. 2008. STRADalpha regulates LKB1 localization by blocking access to importin-α and by association with Crm1 and exportin-7. Mol Biol Cell 19:1614–1626.

Fried H, Kutay U. 2003. Nucleocytoplasmic transport: taking an inventory. Cell Mol Life Sci 60:1659–1688.

Gousias K, Becker AJ, Simon M, Niehusmann P. 2012. Nuclear karyopherin a2: a novel biomarker for infiltrative astrocytomas. J Neurooncol 109:545–553.

Grunwald M, Lazzaretti D, Bono F. 2013. Structural basis for the nuclear export activity of importin13. EMBO J 32:899–913.

Guttler T, Gorlich D. 2011. Ran-dependent nuclear export mediators: a structural perspective. EMBO J 30:3457–3474.

Hanz S, Perlson E, Willis D, Zheng JQ, Massarwa R, Huerta JJ, Koltzenburg M, Kohler M, van-Minnen J, Twiss JL, Fainzilber M. 2003. Axoplasmic importins enable retrograde injury signaling in lesioned nerve. Neuron 40:1095–1104.

Hardie DG, Scott JW, Pan DA, Hudson ER. 2003. Management of cellular energy by the AMP-activated protein kinase system. FEBS Lett 546:113–120.

Hosokawa K, Nishi M, Sakamoto H, Tanaka Y, Kawata M. 2008. Regional distribution of importin subtype mRNA expression in the nervous system: study of early postnatal and adult mouse. Neuroscience 157:864–877.

Jiang Z, Zhang Y, Chen XQ, Lam PY, Yang H, Xu Q, Yu AC. 2003. Apoptosis and activation of Erkl/2 and Akt in astrocytes postischemia. Neurochem Res 28:831–837.

Koch P, Bohlmann I, Schafer M, Hansen-Hagge TE, Kiyoi H, Wilda M, Hameister H, Bartram CR, Janssen JW. 2000. Identification of a novel putative Ran-binding protein and its close homologue. Biochem Biophys Res Commun 278:241–249.

Kortvely E, Burkovics P, Varszegi S, Gulya K. 2005. Cloning and characterization of rat importin 9: implication for its neuronal function. Brain Res Mol Brain Res 139:103–114.

Kutay U, Hartmann E, Treichel N, Calado A, Carmo-Fonseca M, Prehn S, Kraft R, Gorlich D, Bischoff FR. 2000. Identification of two novel RanGTP-binding proteins belonging to the importin beta superfamily. J Biol Chem 275:40163–40168.

Lee JH, Zhou S, Smas CM. 2010. Identification of RANBP16 and RANBP17 as novel interaction partners for the bHLH transcription factor E12. J Cell Biochem 111:195–206.

Li Q, Li Z, Sun CX, Yu AC. 2002. Identification of transcripts expressed under functional differentiation in primary culture of cerebral cortical neurons. Neurochem Res 27:147–154.

Li Z, Li Q, Sun CX, Hertz L, Yu AC. 2001. Cloning and identification of differentially expressed transcripts in primary culture of GABAergic neurons. Neurochem Res 26:1101–1105.

Lowry OH, Rosebrough NJ, Farr AL, Randall RJ. 1951. Protein measurement with the Folin phenol reagent. J Biol Chem 193:265–275.

Ma L, Roman-Campos D, Austin ED, Eyries M, Sampson KS, Soubrier F, Germain M, Tregouet DA, Borczuk A, Rosenzweig EB, Girerd B, Montani D, Humbert M, Loyd JE, Kass RS, Chung WK. 2013. A novel channelopathy in pulmonary arterial hypertension. N Engl J Med 369:351–361.

Mingot JM, Bohnsack MT, Jakle U, Gorlich D. 2004. Exportin 7 defines a novel general nuclear export pathway. EMBO J 23:3227–3236.

Nagara Y, Tateishi T, Yamasaki R, Hayashi S, Kawamura M, Kikuchi H, Iinuma KM, Tanaka M, Iwaki T, Matsushita T, Ohyagi Y, Kira JI. 2013. Impaired cytoplasmic-nuclear transport of hypoxia-inducible factor-1α in amyotrophic lateral sclerosis. Brain Pathol 23:534–546.

Ohashi K, Ouchi N, Higuchi A, Shaw RJ, Walsh K. 2010. LKB1 deficiency in Tie2-Cre-expressing cells impairs ischemia-induced angiogenesis. J Biol Chem 285:22291–22298.

Sato M, Mizoro Y, Atobe Y, Fujimoto Y, Yamaguchi Y, Fustin JM, Doi M, Okamura H. 2011. Transportin 1 in the mouse brain: appearance in regions of neurogenesis, cerebrospinal fluid production/sensing, and circadian clock. J Comp Neurol 519:1770–1780.

Shaw RJ, Kosmatka M, Bardeesy N, Hurley RL, Witters LA, DePinho RA, Cantley LC. 2004. The tumor suppressor LKB1 kinase directly activates AMP-activated kinase and regulates apoptosis in response to energy stress. Proc Natl Acad Sci U S A 101:3329–3335.

Shaw RJ, Lamia KA, Vasquez D, Koo SH, Bardeesy N, Depinho RA, Montminy M, Cantley LC. 2005. The kinase LKB1 mediates glucose homeostasis in liver and therapeutic effects of metformin. Science 310: 1642–1646.

Tiainen M, Vaahtomeri K, Ylikorkala A, Makela TP. 2002. Growth arrest by the LKB1 tumor suppressor: induction of p21(WAF1/CIP1). Hum Mol Genet 11:1497–1504.

Xu F, Gu JH, Qin ZH. 2012. Neuronal autophagy in cerebral ischemia. Neurosci Bull 28:658–666.

Yang CZ, Li HL, Zhou Y, Chai RC, Zhao R, Dong Y, Xu ZY, Lau LT, Yingge Z, Teng J, Chen J, Yu AC. 2011. A new specialization in astrocytes: glutamate- and ammonia-induced nuclear size changes. J Neurosci Res 89:2041–2051.

Yasuhara N, Shibazaki N, Tanaka S, Nagai M, Kamikawa Y, Oe S, Asally M, Kamachi Y, Kondoh H, Yoneda Y. 2007. Triggering neural differentiation of ES cells by subtype switching of importin-α. Nat Cell Biol 9:72–79.

You P, Peng Z, Wang Y, Tao T. 2013. Expression and subcellular distribution of imp13 are regulated in brain development. In Vitro Cell Dev Biol Anim 49:346–353.

Yu AC, Lau LT. 2000. Expression of interleukin-1 alpha, tumor necrosis factor alpha and interleukin-6 genes in astrocytes under ischemic injury. Neurochem Int 36:369–377.

Yu AC, Schousboe A, Hertz L. 1982. Metabolic fate of ^{14}C-labeled glutamate in astrocytes in primary cultures. J Neurochem 39:954–960.

Yu AC, Hertz E, Hertz L. 1984. Alterations in uptake and release rates for GABA, glutamate, and glutamine during biochemical maturation of highly purified cultures of cerebral cortical neurons, a GABAergic preparation. J Neurochem 42:951–960.

Yu AC, Wong HK, Yung HW, Lau LT. 2001. Ischemia-induced apoptosis in primary cultures of astrocytes. Glia 35:121–130.

Yu AC, Lau AM, Fu AW, Lau LT, Lam PY, Chen XQ, Xu ZY. 2002. Changes of ATP and ADP in cultured astrocytes under and after in vitro ischemia. Neurochem Res 27:1663–1668.

Yu AC, Yung HW, Hui MH, Lau LT, Chen XQ, Collins RA. 2003. Cycloheximide and actinomycin D delay death and affect bcl-2, bax, and Ice gene expression in astrocytes under in vitro ischemia. J Neurosci Res 74:318–325.

Yu AC, Lee YL, Fu WY, Eng LF. 1995. Gene expression in astrocytes during and after ischemia. Prog Brain Res 105:245–253.

Yu AC, Liu RY, Zhang Y, Sun HR, Qin LY, Lau LT, Wu BY, Hui HK, Heung MY, Han JS. 2007. Glial cell line-derived neurotrophic factor protects astrocytes from staurosporine- and ischemia-induced apoptosis. J Neurosci Res 85:3457–3464.

Zhou Y, Li HL, Zhao R, Yang LT, Dong Y, Yue X, Ma YY, Wang Z, Chen J, Cui CL, Yu AC. 2010. Astrocytes express N-methyl-D-aspartate receptor subunits in development, ischemia, and postischemia. Neurochem Res 35:2124–2134.